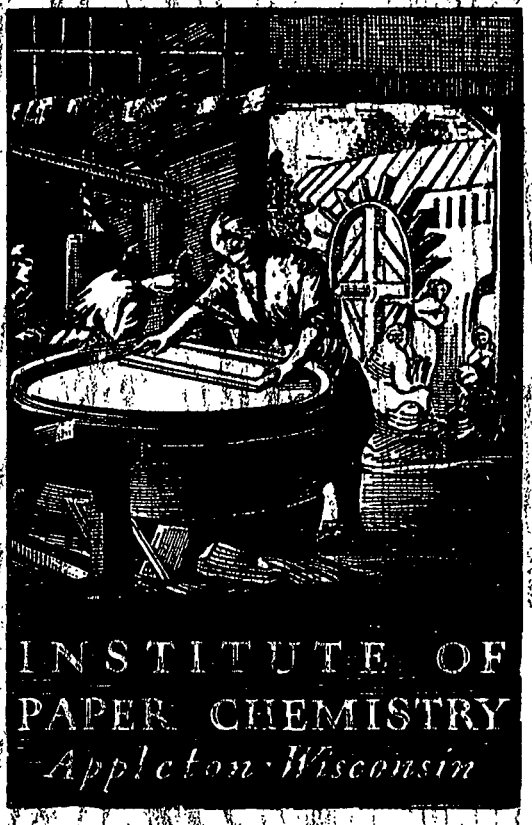

MODEL STUDIES ON FIBER FLOCCULATION

Project 2570

Report One

A Progress Report

to

MEMBERS OF GROUP PROJECT 2570

April 20, 1967

THE INSTITUTE OF PAPER CHEMISTRY

Appleton, Wisconsin

MODEL STUDIES ON FIBER FLOCCULATION

Project 2570

Report One

A Progress Report

to

MEMBERS OF GROUP PROJECT 2570

April 20, 1967

MEMBERS OF GROUP PROJECT 2570:

Allis-Chalmers Manufacturing Company

Appleton Wire Works Corp.

Beloit Corporation

Consolidated Papers, Inc.

Container Corporation of America

Eastman Kodak Company

Fibreboard Corporation

The Glidden Company

International Paper Company

Kimberly-Clark Corporation

Knowlton Brothers

Longview Fibre Company

The Mead Corporation

Oxford Paper Company

Riegel Paper Corporation

Scott Paper Company

Union Camp Corporation

West Virginia Pulp and Paper Company

Weyerhaeuser Company

TABLE OF CONTENTS

THE INSTITUTE OF PAPER CHEMISTRY

Appleton, Wisconsin

MODEL STUDIES OF FIBER FLOCCULATION

SUMMARY

Fiber balls obtained through a manual process and by use of the Jacquelin apparatus were subjected to a Couette-type shear field and their size reduction observed under varying shear rates and as a function of time. The balls always finally disintegrated due to the action of shearing stress, the time of action required being shorter at higher shear rates. A separate study revealed that the initial size of the balls depended on fiber length, and that balls are formed primarily from summerwood fibers.

INTRODUCTION

An introduction to the subject of fiber flocculation as a phenomenon of suspension flow under favorable colloidal conditions is given in the "Critical Review" of "The Status of the Sheet-Forming Process" (1) and reference is made to Chapter XIV of that report. It goes without saying that the deformability of the individual pulp fibers and their irregular shape makes any analytical approach to the flow conditions of fiber agglomeration a hopelessly difficult matter. The chances of understanding this mechanism better would improve, however, if model flocs with manageable but closely related properties could be devised, with a high degree of homogeneity made, and their behavior under defined flow conditions tested both as individuals as well as when suspended in large numbers. Fibrous balls of initially spherical shape have these properties. The study of flow conditions and fluid stress under which they disintegrate would help in the provision of industrial conditions under which full dispersion of the fibers could be approached.

In the abovementioned report (1) reference is made to the results of a preliminary study which suggested that an isolated spherical floc would spin with an angular velocity of

$$\omega = G/2 \tag{1}$$

when G is the velocity gradient in the surrounding flow field, in accordance with what was found earlier for solid spheres (2). It further suggested that there is a relationship between floc size or radius R and the shear rate G of the kind

$$GR^m = f(\sigma_t, a) \tag{2}$$

with σ_t equal to tensile strength and a equal to viscous resistivity of the porous sphere on the grounds that the floc structure while periodically deforming could sustain only those fluid stresses not in excess of its tensile strength. In the following, observations and measurements of fibrous balls of different make and size as made in a Fiber Flexibility Tester (see page 4) are described which to some extent seem to support the idea of floc size-shear rate interdependence. The experimental work performed so far has been to observe: the deformation of a flexible, spherical fiber ball in a shear field, the relationship between the angular velocity of a rotating solid fiber ball and the corresponding shear rate, the flow pattern inside a hollow frame rotating in a shear field, the size reduction of a fiber ball under increasing shear rate, and the size reduction of weak balls as a function of time and shear rate.

All results ought to be looked upon as of a more or less phenomenological nature because of the end effects of the apparatus not accounted for. As far as secondary flow of the Taylor type is concerned, it is true that this type of apparatus is particularly prone to it under ordinary conditions. However, in these studies with single balls suspended in corn sirup, Taylor vortices were apparently absent and, as preliminary tests indicate, they are greatly suppressed even at higher speeds when working with suspensions of balls.

TEST APPARATUS

A Fiber Flexibility Tester, originally developed by The Pulp and Paper Research Institute of Canada and manufactured by Cranemond & Son, Ltd.. Montreal, Canada, was used. A Louis Allis Co. Model 2541-D329-LB Ajusto-Speed Drive was installed in place of the original Zeromax drive to facilitate a single control on both the inner and outer cylinder velocities, as well as a more silent operation with less vibration. Most of the observations were made photographically with a Minolta SR-7 camera and an Ultrablitz Meteor SF electronic flash. Figure 1 shows the apparatus assembled for operation.

Assuming that there are no end effects, Trevelyan and Mason (3) showed that the shear rate at the stationary layer is characterized by the relationship

$$G = \frac{2(R_1^2\omega_1 + R_2^2\omega_2)}{R_2^2 - R_1^2} \qquad (2)$$

where G = shear rate at stationary layer, R_1 = radius of the inner cylinder, R_2 = radius of the outer cylinder, ω_1 = angular velocity of the inner cylinder, and ω_2 = angular velocity of the outer cylinder. A calibration curve of the dial setting of the motor vs. the shear rate is shown in Fig. 2. Trevelyan and Mason also derived an equation relating the location of the stationary layer in the annulus to the speeds of rotation as follows:

$$R_S = R_1 R_2 \sqrt{\frac{N_1 + N_2}{R_1^2 N_1 + R_2^2 N_2}} \qquad (3)$$

where R_S = radius of the stationary layer, R_1 = radius of the inner cylinder, R_2 = radius of the outer cylinder, N_1 = r.p.m. of inner cylinder, and N_2 = r.p.m. of outer cylinder.

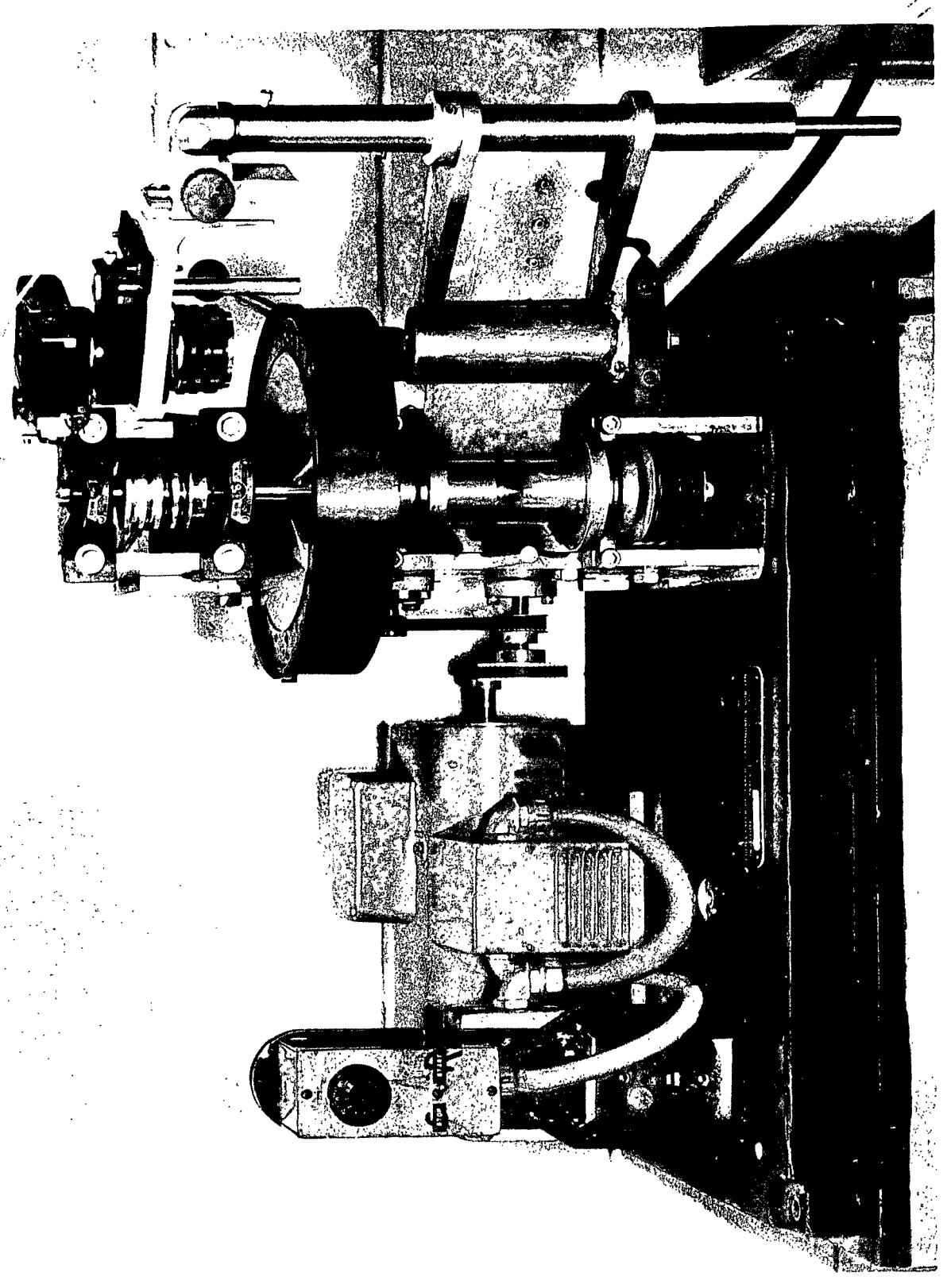

Figure 1. Modified Fiber Flexibility Tester.

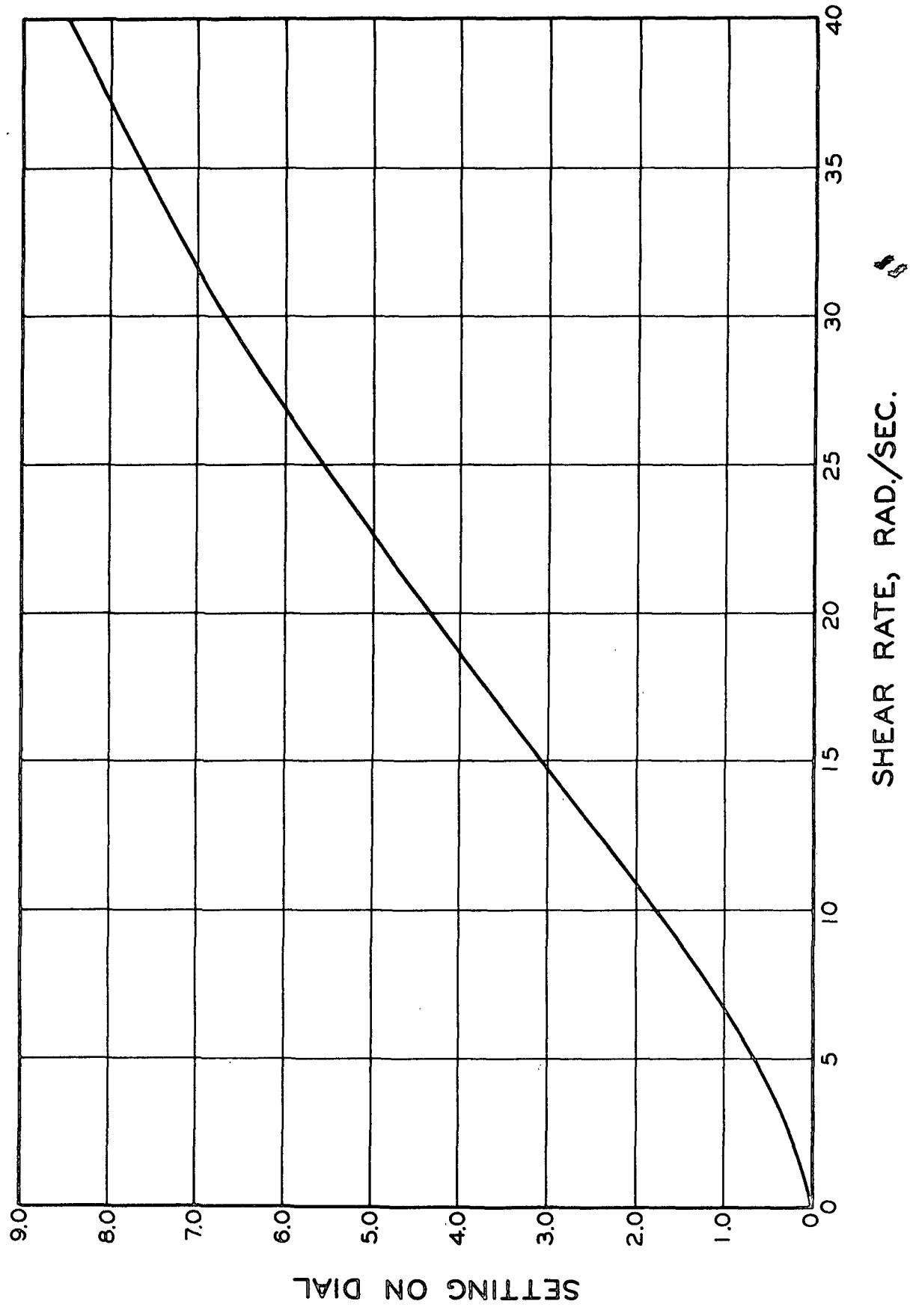

Figure 2. Dial Setting vs. Shear Rate, G.

Equation (4) was used in order to adjust the stationary streamline halfway between cup and bob.

It was found that Karo sirup as a suspending fluid was of desirable specific gravity and viscosity and it was selected to be used as a flow medium in the Flexibility Tester.

THE MAKING OF FIBROUS BALLS

Artificial fiber balls were chosen as the working model for the studies. The fibers used were of Weyerhaeuser bleached sulfite S grade, classified twice on the IPC Web Former equipped with 70 x 56 semitwill wire. The average fiber length was 2.46 mm.

At first difficulties were encountered in forming the fiber balls. Methods such as sedimentation, filtration, molding, and wet rolling were tried and failed either in producing balls of uniform structure or in matching the specific gravity of the flow medium. The manufacturing procedure finally adopted was a tedious one starting with completely dispersed dry fibers which were obtained by disintegrating 2-D sheets made on the IPC Web Former.

Several dry fibers were stuck together with Karo sirup to form a tiny ball. This tiny ball was then rolled upon a very thin layer of dispersed dry fibers to gain size. A very small amount of sirup was then added to the surface of the ball and the rolling process was repeated. As soon as the ball had grown to the desired size, it was taken to the Fiber Flexibility Tester for experiments.

Later, the set-up suggested by Jacquelin (4) was adopted to make fiber balls. Cylindrical containers, 8 in. in diameter by 11 in. long, made of Plexiglas and polyethylene, respectively, were tried out, and each one gave satisfactory results. The containers were set at an angle of 45° and driven by a Zeromax variable-speed motor. Figure 3 shows the arrangement of the apparatus. Several pulps dispersed in distilled water were used to make fiber balls. The results are shown in Table I.

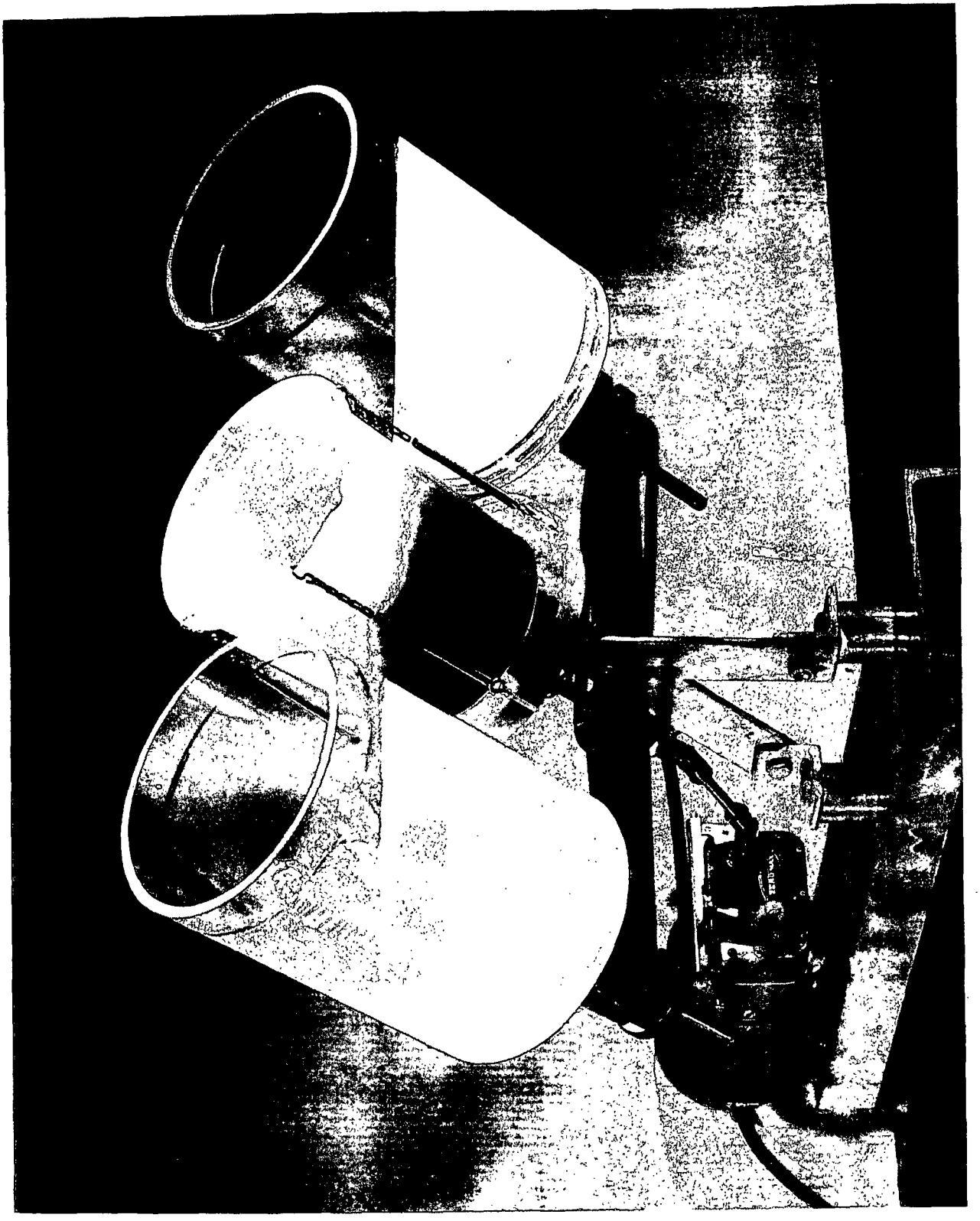

Figure 3. Jacquelin Apparatus.

TABLE I

DATA ON FIBER BALL FORMATION

Fiber	R.p.m.	Container	Time, hr.	Yield, %
Southern pine (unclassified)	50	Plexiglas	28	92
Paraná pine (classified alkaline sulfite)	60	Polyethylene	96	71
Paraná pine (acid sulfite)	40	Polyethylene	96	62
Spruce (sulfite)	50	Plexiglas	96	58
Holopulp (Pinus sylvestris from Finland holocellulose)	60	Plexiglas	24	70

It was noticed that appreciably different sizes of balls were formed within the same batch of pulp, except for the spruce sulfite where the size difference was not quite distinctive. In general, rather round balls were formed, although the time required to start the ball-forming process varied from one pulp to another.

An attempt was made to observe the relationship between the fiber ball size and the fiber length. From each batch except that of the spruce sulfite and the black spruce, "big" balls and "small" balls were picked. In the case of the holopulp, three different grades were picked because of the bigger variation in size. The balls were photographed for the measurement of the average diameter. The same balls were than dispersed, and average fiber lengths were measured. The results are tabulated in Table II and plotted in Fig. 4.

It can be seen from the plot that the fiber ball size and the average length of the fibers that form the balls are very interestingly related: the longer the fibers, the bigger the fiber balls. The straight lines drawn through

TABLE II

FIBER BALL DIAMETERS VS. FIBER LENGTHS

	Ball Diameter, cm.	No. of Balls Picked	Average Fiber Length, cm.
Paraná pine (alk.)			
Big	0.828	5	0.205
Small	0.491	7	0.180
Paraná pine (acid)			
Big	1.062	5	0.280
Small	0.644	7	0.251
Southern pine			
Bag	0.740	6	0.232
Small	0.353	12	0.205
Holopulp			
Size 1	1.057	11	0.230
Size 2	0.589	21	0.200
Size 3	0.467	23	0.187

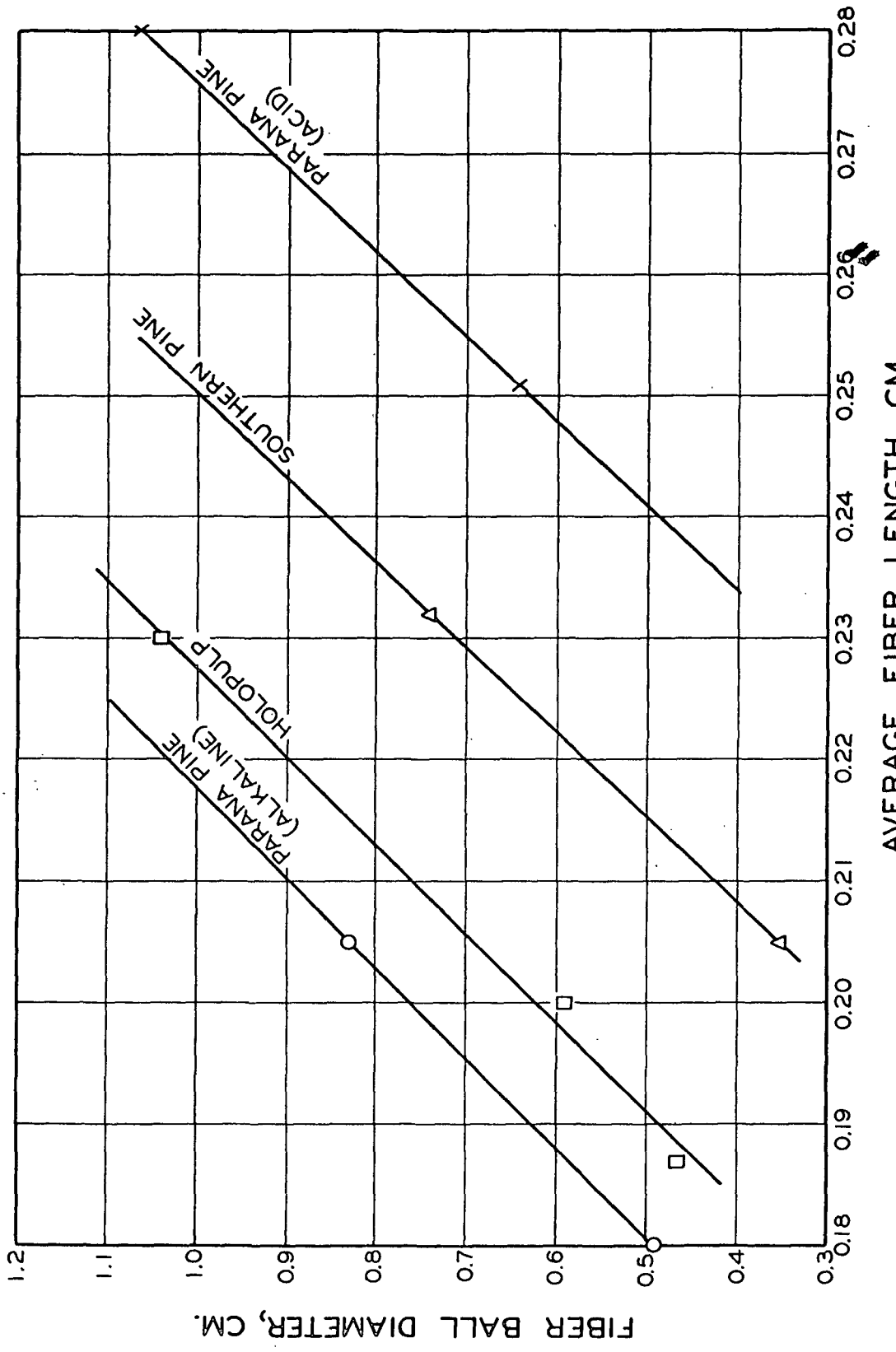

Figure 4, Fiber Ball Diameter Vs. Fiber Length.

the data points are empirical. The fiber characteristics, angular velocity, and the colloidal conditions are probably the factors that would shift the curves upward or downward. No attempts have been made as yet to vary these conditions.

During the fiber ball-forming process, it was observed that certain sequences were followed:

(1) In the early stages of rotation, an increasing number of flocs were formed.

(2) More fibers would be gradually added to the developing flocs while the process of shaping up into spherical flocs or balls was going on. This was evidenced by the fact that the fiber balls grew in size as rotation continued. This speculation concerning the ball-forming process is further supported by the following observations: A batch of Paraná pine kraft pulp was put into the 45°-inclined container after complete dispersion and deaeration. The rotation of the container was set at 60 r.p.m. At certain time intervals samples were taken and the number of shapeless fiber clusters and spherical balls were counted. The results are tabulated in Table III and plotted in Fig. 5.

From these curves it can be seen that the following steps probably have taken place during the ball-forming process: The fibers which are floc forming by nature form clusters quickly, and within a certain time a maximum number of clusters are formed. When this maximum is reached, the clusters start to combine or grow individually into bigger clusters which eventually are shaped into balls as the rotation continues. During this period, the rate of decrease in number of clusters is fast. This is evidenced by the fact that the fiber balls not only increase in number but also in size

Figure 4. Fiber Ball Diameter Vs. Fiber Length.

at the same time. The final stage shows that the number of balls is constant, as it has to be, and the number of clusters drops to zero. The sizes of the fiber balls are, of course, governed by the fiber lengths, angular velocity of the rotating container, and probably other factors.

TABLE III

FLOCCULATION AS A FUNCTION OF TIME

Time, hr.	Number of Clusters	Number of Balls	Time, hr.	Number of Clusters	Number of Balls
0	0	0	28	153	205
1/2	265	0	29	145	199
1	455	0	30	141	196
2	473	0	31	130	190
3	450	0	32	116	197
4	449	0	33	95	227
5	394	44	34	65	205
6	384	71	35	69	214
7	390	79	36	44	202
8	347	91	37	39	225
9	352	108	38	31	234
10	315	119	39	27	226
11	335	131	40	31	212
12	320	121	41	22	208
13	323	130	42	26	214
14	296	146	43	28	228
15	294	142	44	-	230
16	295	148	45	-	215
17	282	164	46	-	224
18	258	167	47	-	210
19	273	171	48	-	207
20	228	192	49	-	227
21	230	170	50	-	227
22	197	200	51	-	216
23	190	182	52	-	224
24	188	192	53	-	210
25	165	185	54	-	211
26	166	190	55	-	230
27	159	210	56	-	232

It would be of revealing interest if one could analyze the flow of a fluid when bound by the walls of an inclined cylinder and by a horizontal free surface as in the Jacquelin apparatus. Eye observation alone does not

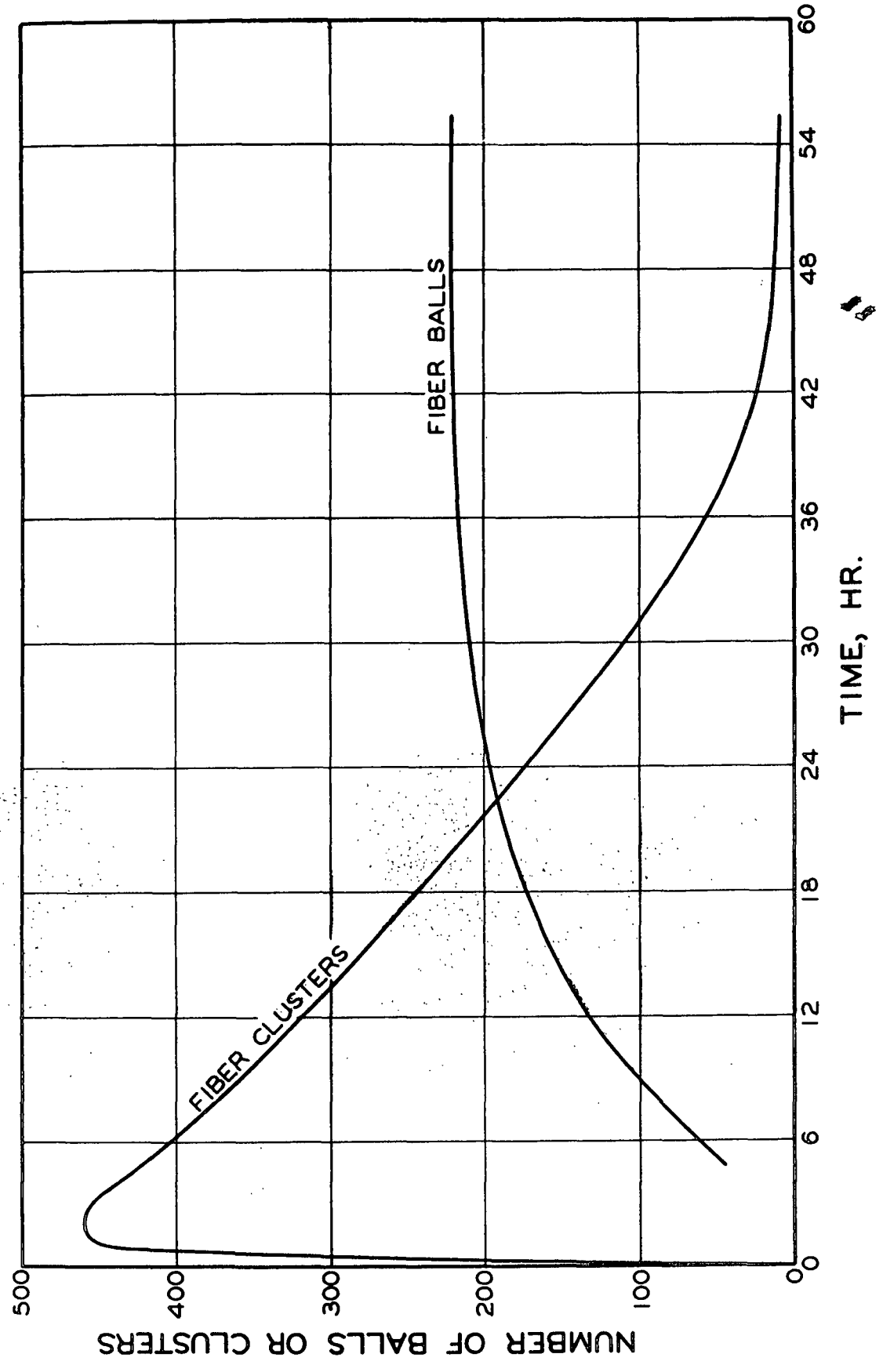

Figure 5. Flocculation as a Function of Time.

show clearly that there may be a region of flow particularly favorable for the forming of balls. The analysis of the flow field would help in locating such a region and in understanding the mechanical conditions both of this particular case and of more general flocculation phenomena. Such an attempt would encounter appreciable problems and remains to be undertaken.

FLOW BEHAVIOR OF SPHERICAL BALLS

Solid fiber balls were used for the observation of the relationship between angular velocity and wall size at different shear rates in order to see whether or not the wall effect is appreciable. The solid balls were handmade of the Weyerhaeuser C-grade bleached sulfite fibers, but were coated with a very thin layer of Duco household cement. In some cases "hollow" balls were used, thus simulating to the extreme a very porous structure. These hollow balls were formed with "skin" made of the same materials as were used for the solid balls. The ball was suspended in the Karo sirup and a series of shear rates were applied. At each shear rate, the number of revolutions made by the ball was recorded. The results are shown in Table IV.

A mixture of the Karo sirup and ink was injected into the space inside the "hollow" ball for showing the flow pattern inside. The ball was immediately suspended at the stationary layer of the Flexibility Tester. A picture taken of the flow pattern inside the hollow ball is shown in Fig. 6. The structure, about 1 cm. in diameter, is approximately 1-1/2 cm. below the surface. As evidenced by a great number of pictures of similar flows about solid and porous balls, the streaks are true images of streamlines. Water in the sirup is probably causing the dilatational effect. The contour of a central core belongs to the dye-sirup mixture which survived for a period of about 5 minutes. This indicates that inside a loose structure like this, relative flow is considerable. As concerning the rotation of the balls, the data indicate no systematic trend. A wall effect is certainly present but may be obscured by using the value of shear rate according to Equation (3) as the theoretical value of shear rate.

TABLE IV

COMPARISON OF MEASURED AND CALCULATED ANGULAR VELOCITIES

Cup Velocity, No. of Rounds/Time, sec.	Bob Velocity, No. of Rounds/Time, sec.	Ball Velocity: Observed No. of Rounds/Time, sec.	Ball Velocity: Observed Angular Velocity, ω	Ball Velocity: Calculated Angular Velocity, ω_c	Ball Velocity: Angular Velocity Ratio ω/ω_c
Run IA - Hollow Ball, diameter = 1.366 cm.					
1/37.75	1/26.45	4/31.7	0.793	0.850	0.933
2/33.5	2/23.8	10/34.1	1.843	1.903	0.969
5/51.4	5/36.45	10/39.2	3.206	3.104	1.03
5/35.4	5/25.1	25/33.45	4.696	4.508	1.04
5/25.9	5/18.2	30/29.6	6.368	6.187	1.03
5/19.3	5/13.5	40/29.5	8.520	8.321	1.02
5/14.3	5/10.05	100/51.0	11.403	11.211	1.02
Run IB - Solid Ball No. 1, diameter = 1.371 cm.					
1/40.1	1/28.8	5/40.25	0.781	0.791	0.987
1/17.1	1/12.1	10/34.9	1.800	1.868	0.964
3/31.1	3/22.1	10/20.6	3.050	3.075	0.992
3/21.25	3/15.0	40/53.35	4.702	4.515	1.04
5/25.6	5/18.0	20/18.65	6.738	6.258	1.08
5/19.1	5/13.5	30/20.85	9.041	8.367	1.08
5/14.1	5/9.95	60/30.2	12.483	11.342	1.10
Run IC - Solid Ball No. 2, diameter = 1.024 cm.					
1/39.6	1/28.6	5/40.7	0.772	0.794	0.972
2/34.3	2/24.25	20/9.25	1.835	1.863	0.985
2/20.75	2/14.45	20/39.85	3.153	3.102	1.02
5/35.4	5/25.1	30/39.9	4.724	4.508	1.05
5/25.65	5/18.2	30/28.6	6.591	6.219	1.06
5/19.25	5/13.5	30/21.1	8.933	8.332	1.07
5/14.2	5/10.05	40/20.65	12.171	11.247	1.08

TABLE IV (Contd.)

Cup Velocity, No. of Rounds/Time, sec.	Bob Velocity, No. of Rounds/Time, sec.	Ball Velocity: Observed No. of Rounds/Time, sec.	Ball Velocity: Observed Angular Velocity, ω	Ball Velocity: Calculated Angular Velocity, ω_c	Ball Velocity: Angular Velocity Ratio, ω/ω_c
Run ID - Solid Ball No. 3, diameter = 0.875 cm.					
2/72.8	2/51.7	5/37.15	0.846	0.876	0.966
2/37.15	2/26.4	10/36.35	1.729	1.716	1.01
3/36.15	3/25.75	15/34.45	2.736	2.643	1.04
5/43.1	5/30.6	25/39.15	4.012	3.700	1.08
5/32.9	5/23.2	30/35.8	5.265	4.863	1.08
5/25.35	5/17.9	50/45.5	6.905	6.307	1.09
5/20.1	5/14.2	50/35.9	8.751	7.952	1.10
5/16.15	5/11.5	50/28.95	10.852	9.861	1.10
10/25.3	10/17.8	50/22.0	14.280	12.660	1.13
Run IE - Solid Ball No. 4, diameter = 0.782 cm.					
1/39.9	1/28.5	8/66.4	0.757	0.797	0.950
2/44.3	2/32.0	10/47.5	1.323	1.428	0.927
3/45.3	3/32.2	20/64.9	1.936	2.111	0.917
5/54.7	5/38.9	30/70.9	2.659	2.913	0.913
5/43.4	5/31.15	30/56.55	3.333	3.656	0.912
5/34.9	5/24.85	40/60.3	4.168	4.563	0.913
5/28.45	5/20.2	50/60.8	5.167	5.605	0.922
5/23.6	5/16.9	60/60.6	6.221	6.730	0.924
5/19.9	5/14.1	60/49.9	7.555	8.021	0.942
6/20.0	6/14.3	60/42.0	8.976	9.537	0.941

Table IV (Contd.)

Cup Velocity, No. of Rounds/Time, sec.	Bob Velocity, No. of Rounds/Time, sec.	Ball Velocity: Observed No. of Rounds/Time, sec.	Ball Velocity: Observed Angular Velocity, ω	Ball Velocity: Calculated Angular Velocity, ω_c	Ball Velocity: Angular Velocity Ratio, ω/ω_c
Run IF - Solid Ball No. 5, diameter = 0.666 cm.					
1/38.5	1/27.6	5/39.6	0.793	0.825	0.961
1/21.95	1/15.6	4/18.6	1.351	1.452	0.930
3/42.1	3/29.9	30/89.4	2.108	2.272	0.928
3/33.4	3/23.85	30/71.45	2.638	2.857	0.923
3/26.2	3/18.7	30/56.2	3.354	3.643	0.921
5/34.9	5/24.85	40/59.85	4.199	4.563	0.920
5/28.65	5/20.4	60/73.05	5.161	5.559	0.928
5/23.0	5/16.3	45/43.5	6.500	6.939	0.937
5/20.6	5/14.1	60/50.1	7.525	7.877	0.955
Run IG - Solid Ball No. 6, diameter = 0.470 cm.					
1/40.2	1/28.8	5/42.6	0.738	0.790	0.934
1/22.3	1/15.9	6/28.9	1.305	1.427	0.915
2/30.35	2/21.6	9/30.0	1.885	2.099	0.898
3/33.6	3/24.0	20/49.4	2.544	2.840	0.896
5/43.5	5/31.1	20/39.55	3.177	3.654	0.870
5/35.0	5/24.9	20/31.6	3.977	4.552	0.874
5/28.6	5/20.35	20/26.25	4.787	5.570	0.859
5/23.9	5/16.9	20/22.1	5.686	6.824	0.833
5/19.9	5/14.1	40/36.6	6.867	8.021	0.856

Figure 6. Flow Pattern Inside Hollow, Spherical Structure.

Comparatively loose fiber balls of the handmade type were used for the purpose of observing deformation under rotation. It was noticed that the ball would deform and lose fibers while rotating in the stationary layer of the annulus. As soon as it was deformed into an elongated shape, the rotation became more like tumbling. Ultimately, the ball was completely disintegrated. Figures 7a to 7g show the sequence.

For the study of size reduction, fiber balls 1-1.5 cm. in diameter of the handmade type were used at first. A single fiber ball was suspended at the stationary layer of the Fiber Flexibility Tester and a photograph taken to record the original ball size. A low shear rate was then applied and enough time allowed to make sure that the ball reached a constant size. This was checked by taking pictures every 10 minutes for 40 minutes. It was found after the first run that 30 minutes were adequate for each size-reducing process. The shear rate was then raised to a higher level and the corresponding size of ball recorded. This same procedure was repeated again and again until the maximum available shear rate had been applied. The pictures were developed and printed on negative sheets, and the average ball diameter obtained. Figures 8a to 8i show the pictures taken for one run. Three runs were made. The data for the handmade ball are shown in Table V, and plots of log $\underline{R}$ vs. log $\underline{G}$ as suggested by Equation (2) are given in Fig. 9a, 9b, and 9c. A power law relationship between ball size and shear rate appears thus to be applicable at least over certain ranges of the size reduction. Variations between the three sets of data may be due to differences in packing density or tensile strength of the balls used.

The behavior of the fiber balls produced in the Jacquelin apparatus was then tested. By comparison, these fiber balls were rather weak in structure and a state of equilibrium size at any shear rate was apparently

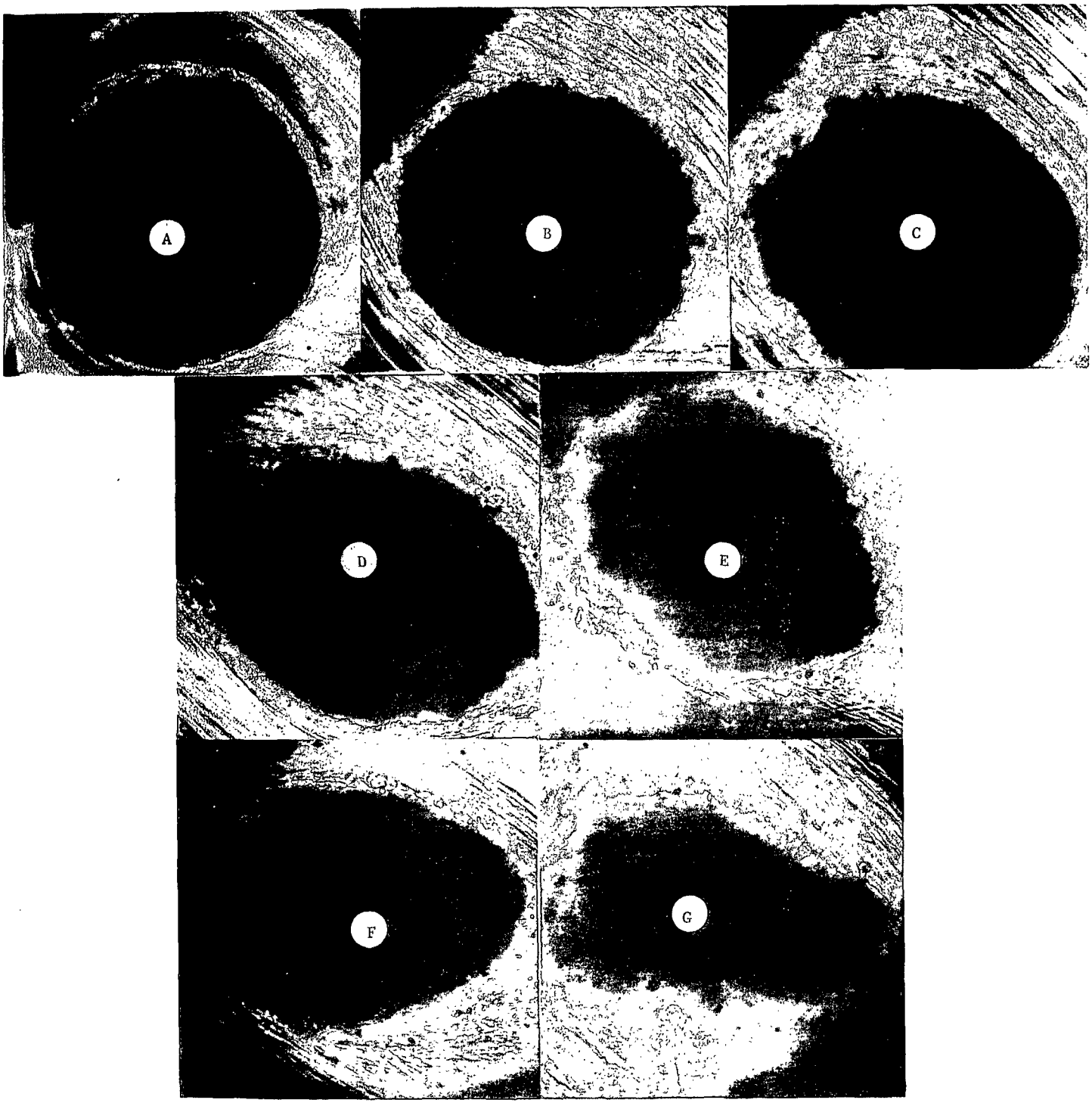

Figures 7a-7g. Disintegration of a Fiber Ball.

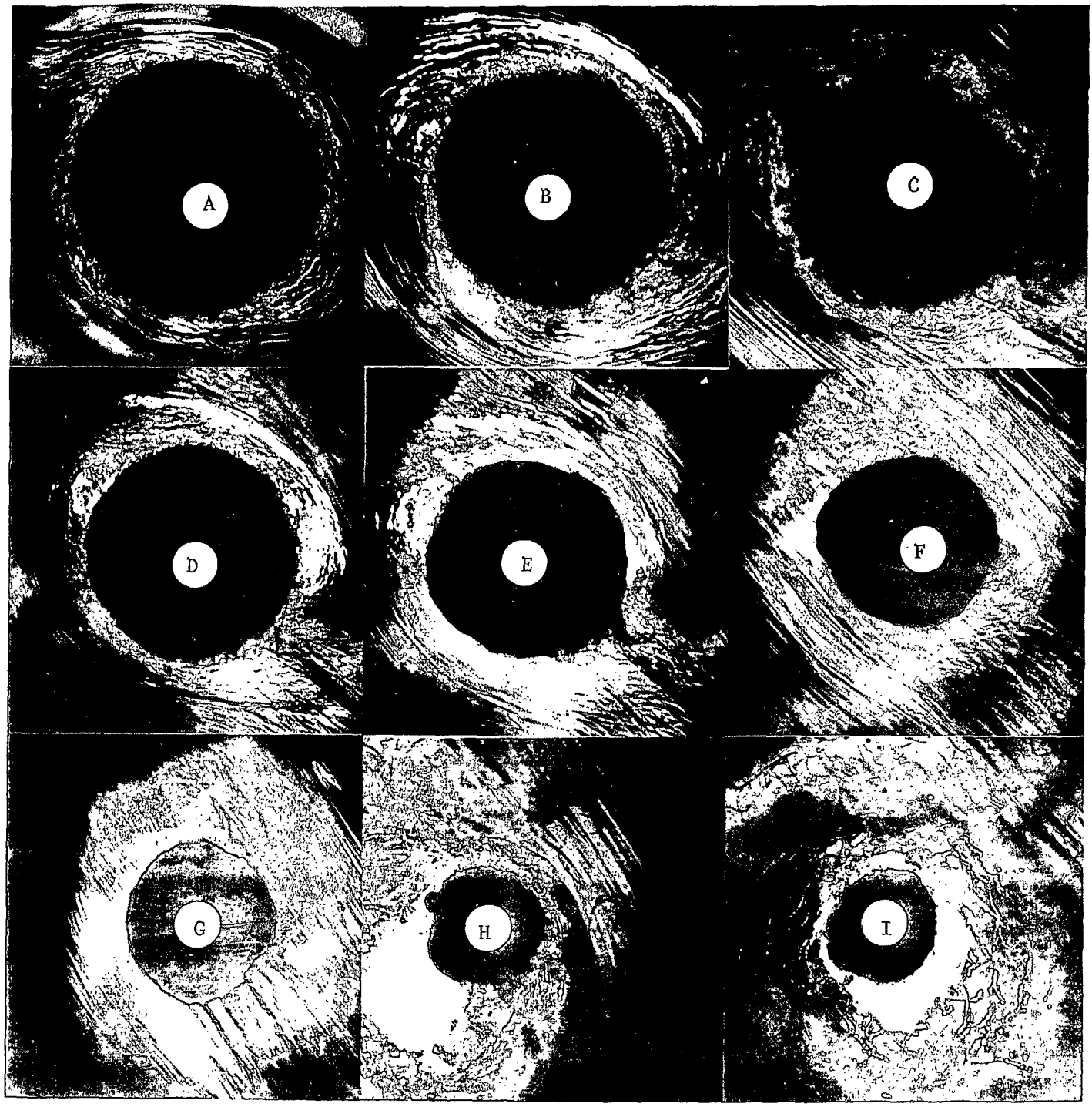

Figures 8a-8i. Size Reduction of a Hand-Made Fiber Ball.

TABLE V

SIZE REDUCTION DATA

(Bob diameter = 3.98 in.; cup diameter = 5.02 in.)

Cup Velocity, No. of Rounds/Time, sec.	Bob Velocity, No. of Rounds/Time, sec.	Shear Rate, G radians/sec.	Average Ball Diameter, R, cm.
		Run II-A	
0	0	0	4.63
1/68.4	1/49.8	0.922	4.69
1/18.8	1/13.3	3.40	4.58
2/22.1	2/15.8	5.75	4.5[illegible]
5/40.45	5/28.85	7.87	4.20
5/30.6	6/26.2	10.40	4.08
8/36.0	10/32.1	14.14	3.88
10/33.85	10/24.1	18.82	3.80
7/17.55	8/14.1	25.56	3.-8
20/35.4	20/25.6	35.73	2.12
		Run II-B	
0	0	0	6.63
1/65.35	1/46.5	0.975	6.52
2/49.1	2/35.1	2.59	6.[illegible]
3/42.5	3/30.5	4.48	6.-5
4/36.3	4/25.9	7.01	6.12
5/32.6	5/23.0	9.81	5.--
5/23.6	5/16.7	13.54	5.-7
7/26.4	7/18.65	16.95	5.08
7/18.3	7/13.1	24.31	3.-5
		Run II-C	
0	0	0	6.[illegible]
5/142.65	5/101.55	2.23	6.[illegible]
2/51.0	2/36.1	2.51	4.99
2/37.15	2/26.4	3.43	4.[illegible]
3/48.85	3/34.8	3.91	3.70
4/47.9	4/34.0	5.33	2.[illegible]
5/43.65	5/30.9	7.32	2.[illegible]
5/30.8	5/21.8	10.37	1.[illegible]
5/23.3	5/16.6	13.67	1.32

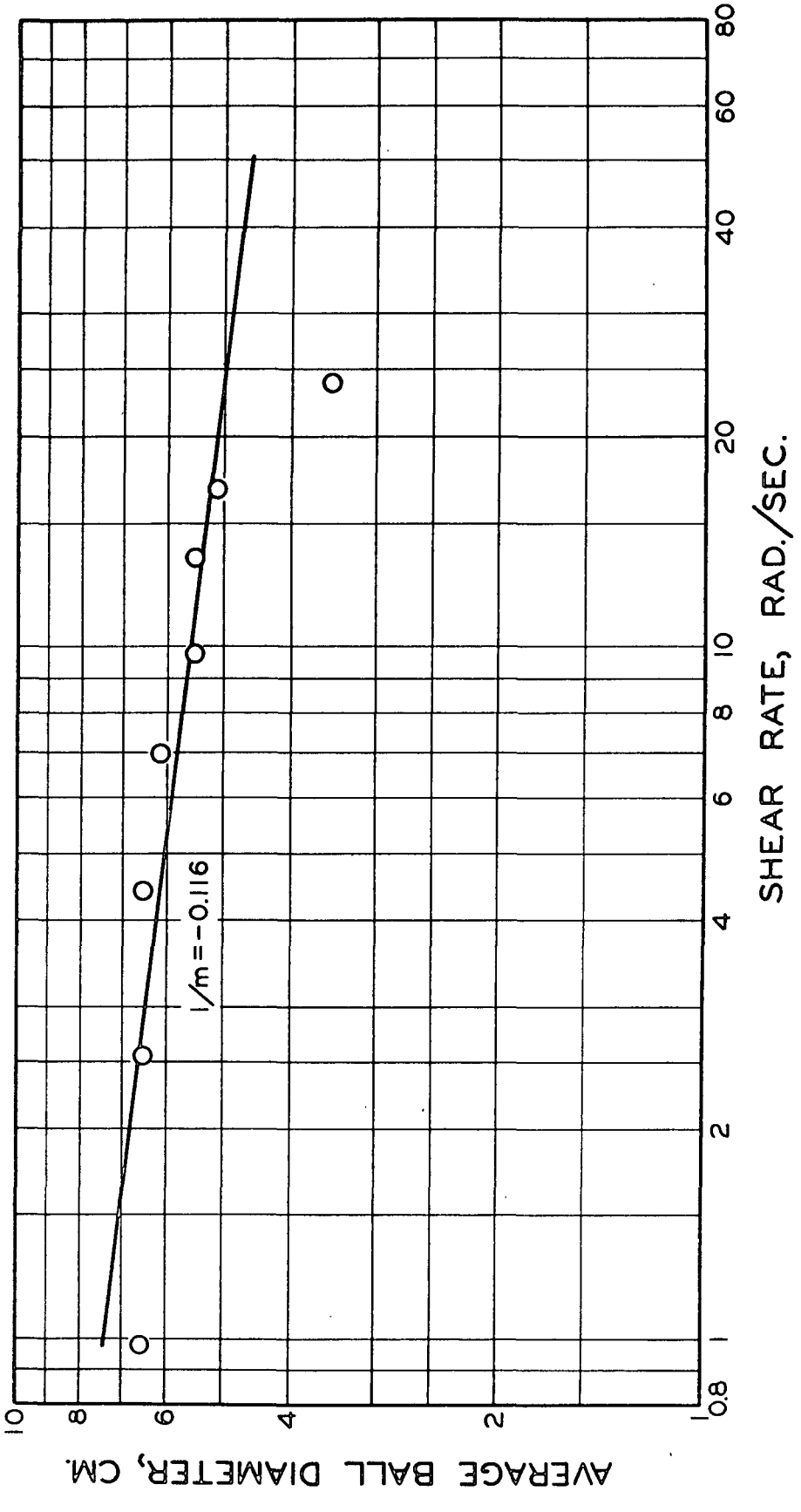

Figure 9a. Ball Diameter as a Function of Shear Rate.

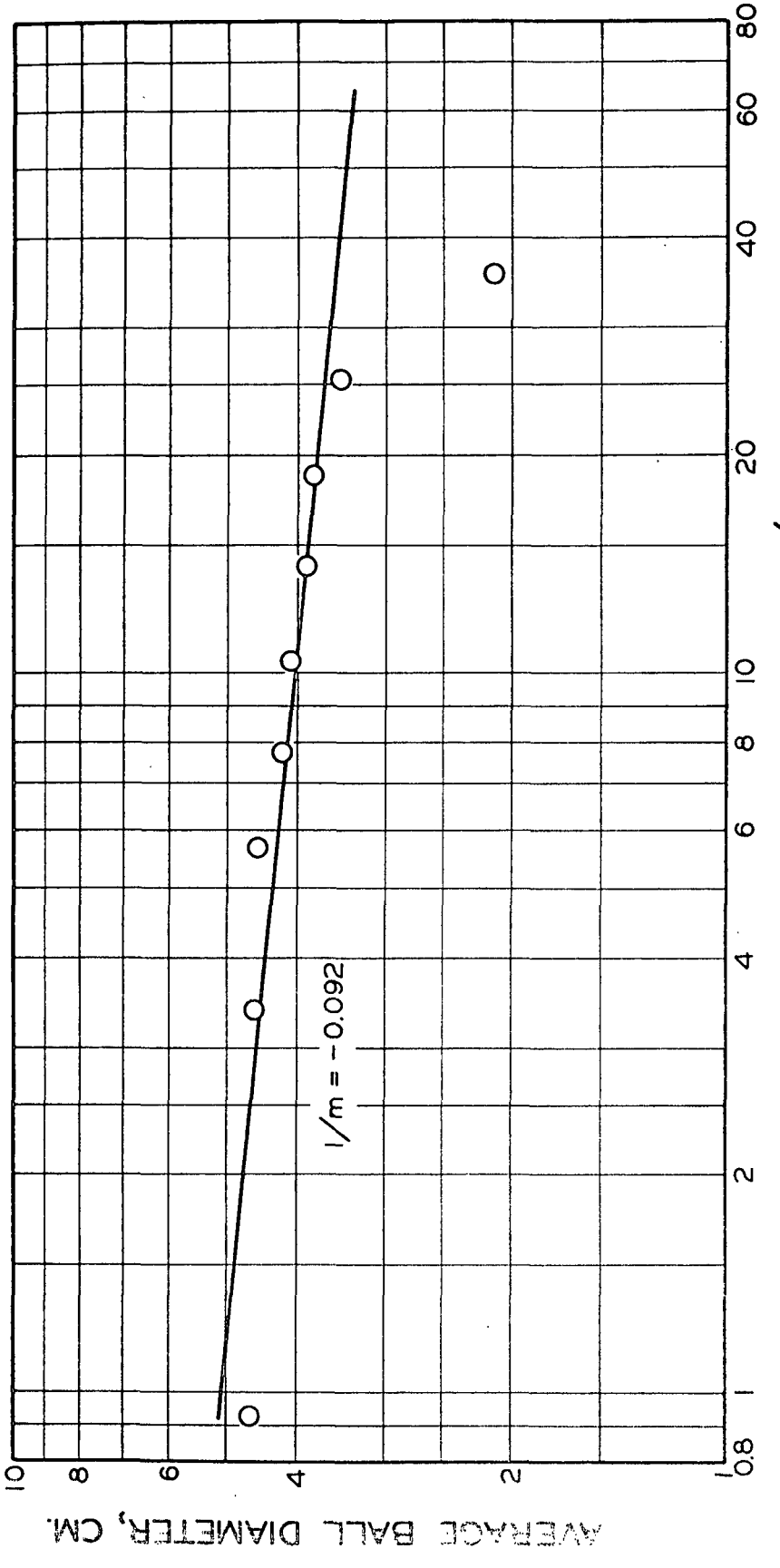

Figure 9b. Ball Diameter as a Function of Shear Rate.

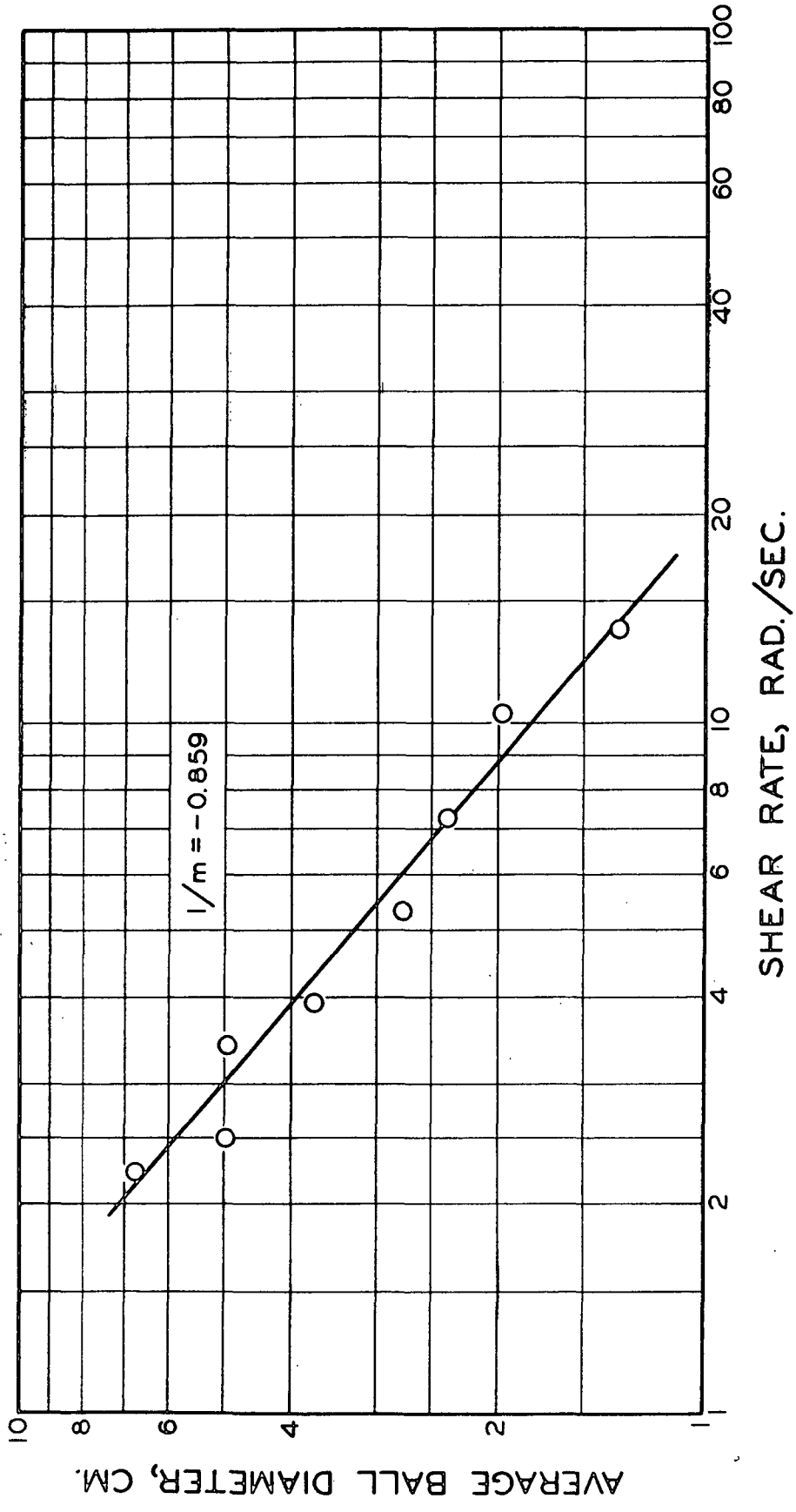

Figure 9c. Ball Diameter as a Function of Shear Rate.

nonexistent. The balls certainly could not resist a shear rate of 11.0 rad./sec. without gradually disintegrating. A series of tests was therefore made to observe the fiber ball size as a function of time for a number of fixed shear rates. The data are tabulated in Table VI and presented graphically in Fig. 10. At any constant shear rate the balls lose few fibers initially but increasingly more in the course of time. Invariably, a point is reached where disintegration sets in rather abruptly. This can be explained by considering the fact that while rotating, the ball is subjected to periodic changes of tension and compression. Thereby the entanglement of the fibers is loosened and the ball structure weakened to an increasing degree. Apparently, its tensile strength decreases with time. Cross plotting of the data in Fig. 10 by making time the parameter results in Fig. 11, where the relative sphere size is plotted as a function of shear rate on log-log coordinates. Straight-line portions ahead of the region of rapid disintegration are fairly well defined, which could be empirically described in terms of power law relationships. The general form of Equation (2) is thus again qualitatively confirmed. However, a much more involved theory than the one underlying that equation would have to be devised in order to include the time effect. Empirically, the time effect could be taken care of by also letting the power m change with time.

TABLE VI

EFFECT OF TIME AND SHEAR RATE ON FIBER BALL SIZE

Shear Rate, rad./sec.	Cumulative Time, min.	Fiber Ball Diameter on Enlarged Photograph, in.
12.5	0	2.613
	23	1.727
	33	1.098
	37	0 (disintegrated)
11.8	0	2.915
	30	2.231
	48	1.738
	60	0
11.8	0	2.967
	30	2.406
	45	1.879
	53	0
11.0	0	2.758
	15	2.529
	30	2.377
	45	2.160
	60	1.838
	78	0
11.0	0	2.592
	15	2.318
	30	2.154
	45	1.971
	75	0.920
	84	0
11.0	0	2.529
	15	2.293
	30	2.262
	45	2.025
	60	1.826
	75	1.309
	82	0

TABLE VI (Contd.)

Shear Rate, rad./sec.	Cumulative Time, min.	Fiber Ball Diameter on Enlarged Photograph, in.
10.2	0	2.621
	15	2.464
	30	2.381
	45	2.281
	60	2.229
	75	2.191
	90	2.139
	105	1.967
	120	1.908
	135	1.865
	150	1.655
	165	1.578
	183	0
10.2	0	2.731
	30	2.412
	90	2.057
	120	1.676
	143	0
10.2	0	2.490
	15	2.371
	30	2.287
	45	2.158
	60	2.043
	75	2.014
	124	1.469
	146	0
10.2	0	2.656
	30	2.356
	60	2.225
	90	2.088
	120	1.943
	150	1.496
	165	1.205
	177	0
9.4	0	2.471
	15	2.381
	30	2.321
	45	2.315
	60	2.285
	75	2.195

TABLE VI (Contd.)

Shear Rate rad./sec.	Cumulative Time, min.	Fiber Ball Diameter on Enlarged Photograph, in.
9.3 (contd.)	105	1.928
	135	1.998
	165	1.736
	180	1.576
	195	1.086
	210	0
9.3	0	2.572
	30	2.291
	60	2.245
	90	2.180
	120	2.027
	150	1.895
	195	1.289
	213	0
8.5	0	2.482
	30	2.356
	60	2.242
	90	2.047
	120	2.033
	150	1.930
	229	1.184
	239	0.971
	247	0
8.5	0	2.807
	105	2.357
	165	2.098
	240	1.231
	255	0
7.6	0	2.631
	60	2.479
	90	2.342
	120	2.377
	150	2.307
	177	2.283
	237	2.191
	252	1.982
	267	1.912
	282	1.922
	297	1.664
	330	0

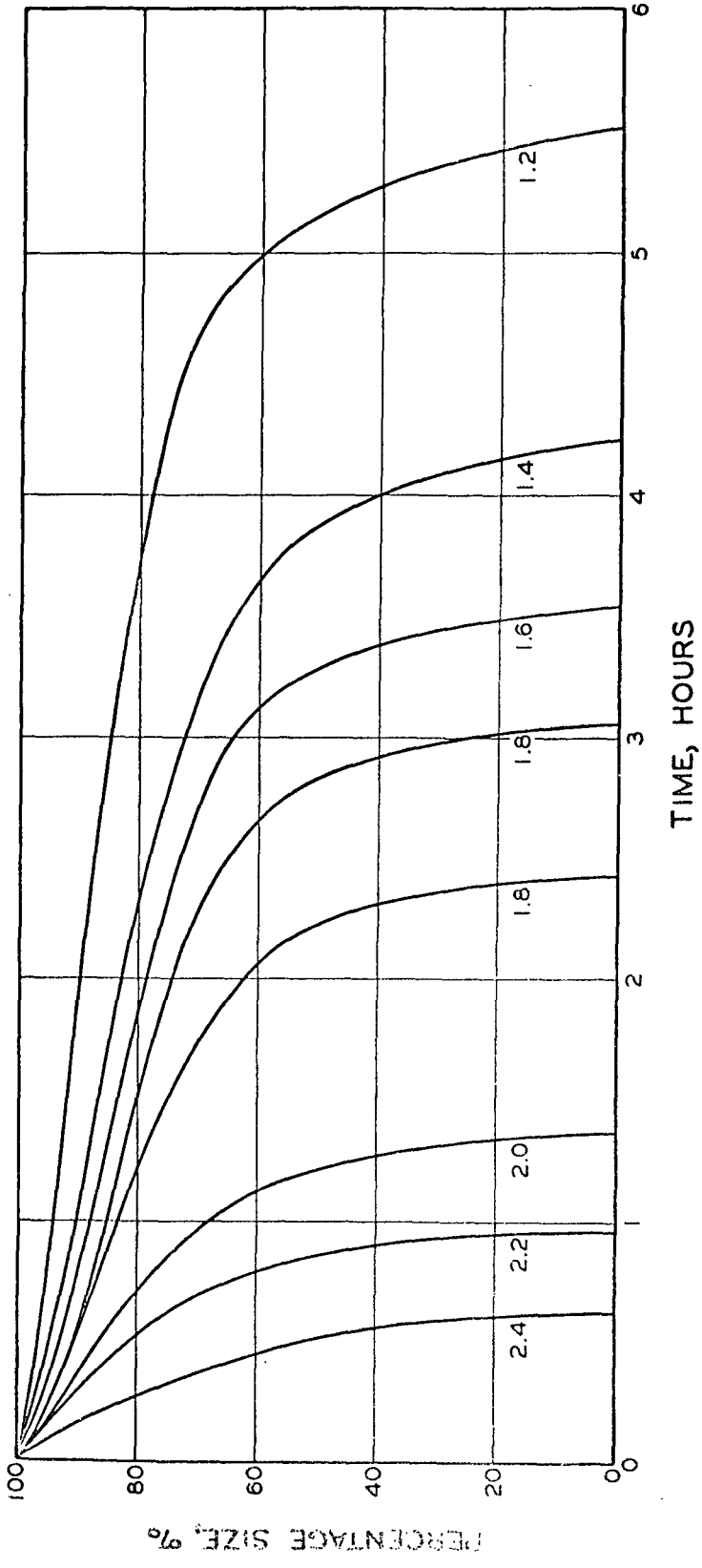

Figure 10. Fiber Ball Size as a Function of Time (Shear Rate as Parameter).

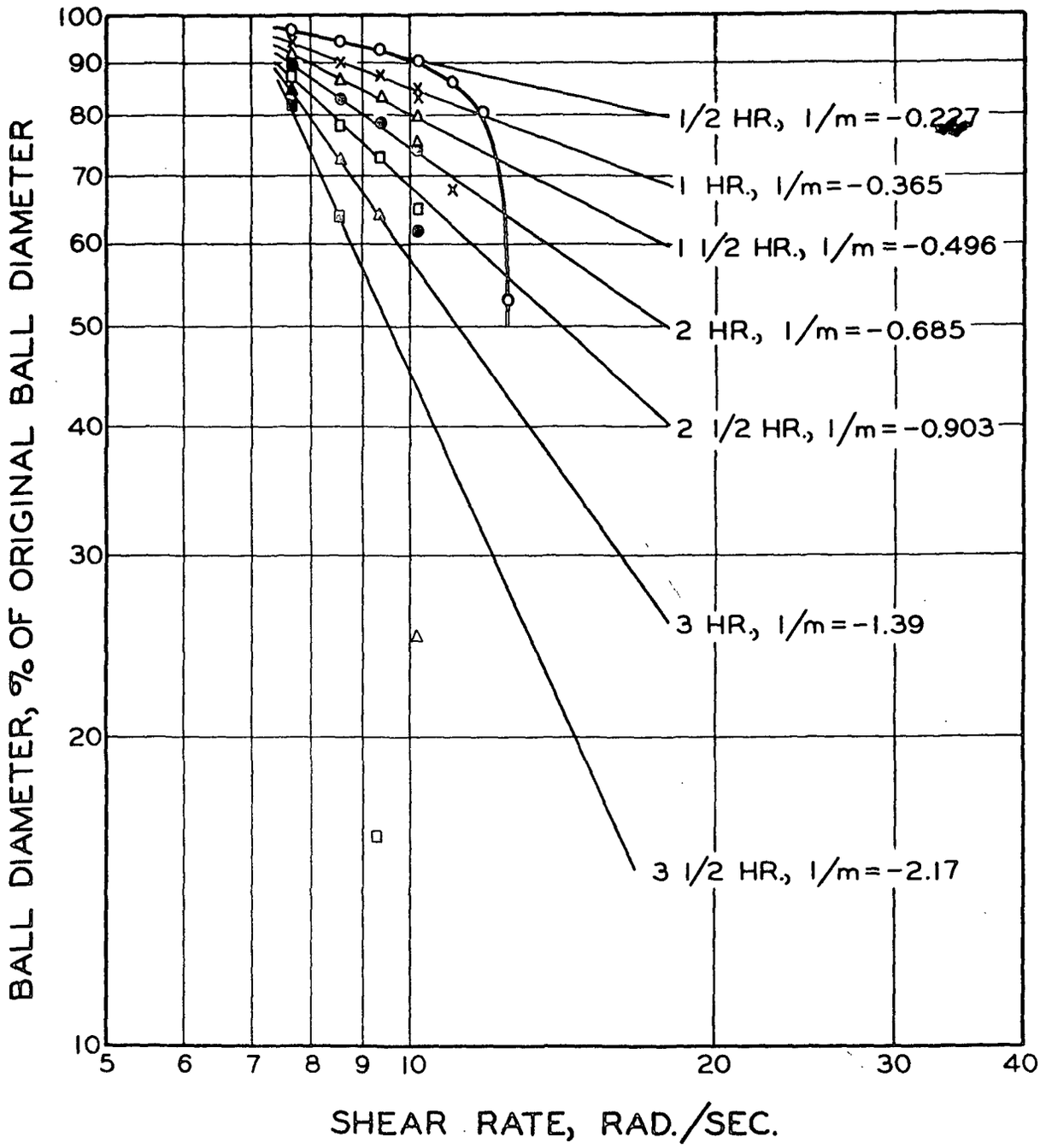

Figure 11. Fiber Ball Size as a Function of Shear Rate (Time as Parameter).

CONCLUSIONS AND FUTURE WORK

Suspension of wood pulp fibers in distilled water in a Jacquelin apparatus form into spherical balls which may be considered as symmetrical flocs. The flow conditions in such an apparatus are peculiar and unknown in detail. When these flocs are exposed to a Couette-type shear field of sufficient strength, their size reduces gradually at first, with a rate of reduction which is proportional to some power of the applied shear rate, and then they disintegrate rather suddenly. Size reduction and final disintegration are due to the work done on the porous structure by fluid stresses. The observations made in the present study are valid for shear fields essentially unaffected by the presence of the porous balls.

The next logical step would be to study the behavior of a suspension of balls under identical geometric conditions and at a concentration wherein the overall flow will be affected by the presence of the balls. In observing the size reduction process under such conditions, the goal would be an understanding of how the combination of collisions, contacts, and fluid flow relative to the porous structures change ordinary flow into a non-Newtonian pattern. Undoubtedly, the insight gained in dealing with the spherical models of natural flocs can be applied profitably to the understanding of the flow behavior of naturally flocculated fibrous suspensions and may help in the design of mechanical conditions for the control of flocculation prior to the forming of a sheet.

NOMENCLATURE

$\underline{G}$ = shear rate at stationary layer, rad./sec.

$\underline{N_1}$ = speed of the inner cylinder, rounds per minute

$\underline{N_2}$ = speed of the outer cylinder, rounds per minute

$\underline{R}$ = particle diameter, cm.

$\underline{R_1}$ = radius of the inner cylinder, in. or cm.

$\underline{R_2}$ = radius of the outer cylinder, in. or cm.

$\underline{R_s}$ = radius of the stationary layer, in. or cm.

$\underline{a}$ = viscous resistivity of porous sphere, consistent unit

$\underline{m}$ = size reduction parameter, dimensionless

$\underline{\sigma_t}$ = tensile strength, consistent units

ω = angular velocity, rad./sec.

ω_1 = angular velocity of inner cylinder, rad./sec.

ω_2 = angular velocity of outer cylinder, rad./sec.

ACKNOWLEDGMENT

The authors wish to acknowledge the assistance of Mr. O. C. Kuehl in the modification of the Fiber Flexibility Tester and the construction of the Jacquelin apparatus, and of Mr. H. H. Heller for differentiating the springwood and summerwood fibers and interpreting the results of the handsheet properties.

LITERATURE CITED

1. Han, S. T. The status of the sheet-forming process--a critical review Appleton, Wisconsin, The Institute of Paper Chemistry, 1965.

2. Nawab, M. A., and Mason, S. G., J. Phys. Chem. 62:1248(1958).

3. Trevelyan, B. J., and Mason, S. G., J. Colloid Sci. 6:354(1951).

4. Jacquelin, G., Tech. Rech. Papet. 7:22-36(March, 1966).

THE INSTITUTE OF PAPER CHEMISTRY

N. L. Chang
Research Fellow
Technology Section

H. Meyer
Research Associate
Technology Section

APPENDIX I

SPRINGWOOD-SUMMERWOOD DIFFERENTIATION

Jacquelin (4) observed that in coherent flocs or balls, thick-walled fibers dominated, whereas thinner walled fibers were concentrated in the suspension.

Agreement with Jacquelin was obtained when Coosa pine pulp and Parana pine kraft pulp were experimented for the springwood and summerwood differentiation. The Coosa pine pulp was rotated in the container for 24 hr. The fiber balls were picked out and washed. Slides were made of the dispersed fiber balls (hereafter designated "B") and the unballed fibers (hereafter designated "F"), respectively. Two sets of three slides each containing F,F,B and F,B,B, respectively, were prepared. Eight persons were invited to examine the slides under the microscope and pick out the odd ones. One observer failed to pick out the odd one correctly in the F,F,B group, and all observers chose correctly in the F,B,B, group.

If the "B" fibers were indistinguishable from the "F" fibers, it could be shown that the probability of eight or seven persons picking correctly would be 0.0152 and 0.244%, respectively. But under the microscope it can easily be seen that summerwood fibers, which are narrower, thick walled, and more rigid, comprised the great majority of fibers constituting the balls, while those remaining in the dispersed form were mainly springwood fibers. From the above statistical result it is concluded that there is a significant difference between the ball-forming and -nonforming fibers.

Another test was made with the Parana pine pulp. This pulp was chosen because under the microscope the summerwood and springwood fibers look more alike. This, of course, would make the test more difficult for

the observers. This test was conducted in a similar way except that the balled fibers and unballed fibers were "purified" once more. The fiber balls were dispersed and rotated to form balls again. The balls thus formed were designated B-B, while the unballed fibers were called F-B. Similarly, the unballed fibers from the first separation were rotated to form balls. The balls thus formed were designated B-F, while the unballed fibers were called F-F. One group of slides consists of B-B, B-B, and F-F fibers and the other group of F-F, F-F, and B-B fibers. One observer failed to pick out the odd one correctly in the latter group, and all observers chose correctly in the former group.

Comparison was then made on the properties of the handsheets made of the B-B and F-F fibers, respectively. Coosa pine and Paraná pine were used. The results are tabulated in Table VII.

TABLE VII

HANDSHEET PROPERTIES

	Coosa Pine		Parana Pine	
	B-B	F-F	B-B	F-F
Av. basis weight, g./m.^{2}	60.0	60.1	60.3	56.9
Thickness, microns	121	107	139	125
Density, g./cc.	0.469	0.562	0.434	0.455
Burst factor	6.03	22.2	13.5	28.7
Tear factor	120	216	269	439
Breaking length, m.	1650	3540	2780	4350

It can be seen that the handsheets made of springwood fibers (F-F) have remarkably higher strength, not only in burst and tensile but also in tear. This is probably due to the following reasons:

(a) The walls of springwood fibers are thinner and more collapsible. In forming sheets, this means more contact area between fibers. Assuming the same H-bonding can be obtained from both springwood and summerwood fibers, the former should form stronger sheets.

(b) The springwood fibers are subject to more swelling. This conclusion is based upon the fact that under the microscope, a higher degree of fibrillation is observed in the case of springwood fibers. This means higher specific surface and higher strength of the handsheets.

(c) The number of fibers per unit weight of springwood fibers is expected to be higher than that of the summerwood fibers. This eventually leads to more contact area and stronger sheets of the same weight.